

Reactions in Elastomeric Nanoreactors Reveal the Role of Force on the Kinetics of the Huisgen Reaction on Surfaces

Xu Han,[†] Shudan Bian,[†] Yong Liang,[‡] K. N. Houk,[‡] and Adam B. Braunschweig^{*,†}

[†]Department of Chemistry, University of Miami, Coral Gables, Florida 33146, United States

[‡]Department of Chemistry and Biochemistry, University of California, Los Angeles, Los Angeles, California 90095, United States

S Supporting Information

ABSTRACT: The force dependence of the copper-free Huisgen cycloaddition between an alkyne and a surface-bound azide was examined in elastomeric nanoreactors. These studies revealed that pressure and chain length are critical factors that determine the reaction rate. These experiments demonstrate the central role of pressure and surface structure on interfacial processes that are increasingly important in biology, materials science, and nanotechnology.

The velocities of reactions in solution k are accelerated at a rate proportional to their activation volume V^\ddagger and the applied pressure P according to a relation first described by Van't Hoff (eq 1).¹

$$\left(\frac{d \ln k}{dP}\right)_T = \frac{-V^\ddagger}{RT} \quad (1)$$

The effect of isotropic pressure on reactions in solution is now well established,^{2–4} and the ability of anisotropic shearing forces to induce predictable bond cleavage in molecules with mechanically responsive functional groups has become the focus of considerable interest because of their utility in stimuli responsive materials.^{4–10} Only recently have studies on the role of isotropic force been extended to include mechanically induced bond formation,^{11–17} which could be used to covalently pattern molecules onto surfaces, leading to breakthroughs in biosensing, molecular electronics, and the understanding of reactivity at interfaces. To this end, we have lately demonstrated the first method to covalently pattern graphene by employing a force-accelerated Diels–Alder reaction that does not proceed in the absence of applied pressure.¹⁸ However, the mechanisms by which force accelerates surface reactions remains poorly understood, because there are few experimental methods capable of controlling precisely critical reaction parameters such as reaction time t and applied P . Forces can be controlled accurately using a single AFM tip,^{19–22} but the low throughput of this method necessitates complex single-molecule analyses. Alternatively soft lithography has been used to investigate force-accelerated reactions over large areas,^{23–25} which simplifies analysis, but the applied P is difficult to control. As a result, these AFM and soft lithography experiments can lead to inconsistent and contradictory results. For example, attempts to use force to induce the Huisgen cycloaddition reaction between alkyne-terminated surfaces and azide substrates, or vice versa, in the

absence of Cu^I have alternately concluded that the reaction does^{23,25} and does not²⁴ proceed under applied pressure. Before the potential of force-induced reactions on surfaces can be realized, there is a need for new experimental methods that can deliver soft organic and biologically active materials onto a surface, apply a controlled localized force, and print over large areas with micrometer scale resolution.

We report how arrays composed of approximately 10,000 elastomeric tips^{26–28} mounted on the piezoactuators of an atomic force microscope (AFM) can be used to apply a localized force that accelerates the Huisgen 1,3-dipolar cycloaddition reaction between azide-terminated monolayers and alkyne inks in the absence of the Cu^I catalyst. Upon bringing the tips into contact with the surfaces, a nanoreactor is formed between the tips and the surfaces that confines the reactants under an applied force (Figure 1). Several aspects of this approach are ideal for patterning applications and for understanding how force and interface structure contribute to the rate constant of reactions, namely (1) these tip arrays uniformly deposit delicate organic and biologically active materials onto surfaces,^{29,30} (2) the piezoelectric tip actuation provides precise control over reaction time and the applied force between the tips and the substrates,

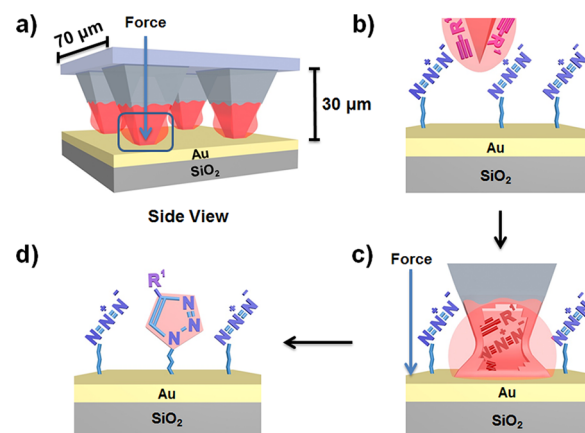


Figure 1. (a) Elastomeric tip array coated with an ink mixture consisting of alkyne and PEG (red) printing onto an azide-terminated Au surface. (b) Magnified view of the inked tip array approaching the surface. (c) Tip forms a nanoreactor with the surface by applying a force that accelerates the Huisgen cycloaddition reaction. (d) After washing, only covalently bound molecules remain on the surface.

Received: April 25, 2014

Published: July 16, 2014

and (3) the large patterns (cm^2) created by the massively parallel tip arrays facilitate fluorescence microscopy and electrochemical analysis of the surface reactions. In these studies we show that the rate constant k of the Huisgen reaction on surfaces is sensitively dependent on applied force and, surprisingly, the alkyl chain length of the azide-terminated monolayer.

The ability of compressive force to induce the Huisgen reaction was investigated by printing fluorescent **1** and redox-active **2** alkyne inks³¹ onto azide-terminated SiO_2 and Au surfaces, respectively. Previously, we have used these same inks to study the ability of polymer pen lithography^{26,27} to induce the Cu^I catalyzed azide–alkyne click reaction in the absence of applied force and short (<20 s) print times, and we found that under those conditions the reaction does not proceed without the Cu^I catalyst.³² To carry out the printing, molded elastomeric tips composed of polydimethylsiloxane and azide-terminated monolayers on SiO_2 and Au were prepared following reported literature protocols.^{31,32} In a typical experiment, a mixture composed of alkyne (3 mM) and polyethylene glycol (PEG) (2000 g/mol, 5 mg) was dissolved in 1 mL 4:1 EtOH:H₂O, and this mixture was sonicated for 3 min to guarantee solution homogeneity. The pen array was exposed to O₂ plasma to render the surface of the arrays hydrophilic, and the ink mixture was spin coated onto the tip arrays (2000 rpm, 2 min). The PEG is added to the ink mixture to encapsulate the reactive species and ensure uniform transport through the aqueous meniscus that forms between the tips and the surface.³⁰ The tip arrays were mounted onto an AFM specially equipped with a tilting stage to level the pen array, an environmental chamber to control humidity, and a customized lithography software to control the force and contact time between the tips and the surfaces. The forces were varied by changing the extension of the z -piezoactuators holding the tips.^{33,34} Following printing, the surfaces were washed with copious amounts EtOH and H₂O to remove molecules that were not covalently immobilized from the surface.

Initially, bond formation was confirmed by printing fluorescent ink **1** and analyzing the resulting patterns by fluorescence microscopy. In these experiments six different spots were printed by each tip, where t was held constant, the force was varied from 0.29 to 0.42 mN, and printings were repeated at t of 0, 60, 180, 300, 420, and 600 s (Figure 2a). The force was determined by measuring the tip edge length during printing, which can be converted to the applied force following a previously described relation.³³ The fluorescence images ($\lambda_{\text{ex}} = 532\text{--}587$ nm, $\lambda_{\text{em}} = 608\text{--}687$ nm) demonstrate that uniform fluorescent patterns are formed over large areas,³¹ delivering evidence of covalent immobilization. Although the fluorescence data provide only qualitative information on the extent of the reaction, fluorescence signal-to-background increases with both force and t (Figure 2b). As a control experiment, fluorescent ink **1** was printed onto an amine-terminated glass surface at 0.42 mN for 600 s, and no fluorescent pattern was visible after rinsing with EtOH and H₂O, which confirms that both azide and alkyne are required for ink immobilization.

Redox-active ink **2** was subsequently deposited onto Au surfaces coated with a SAM composed of 11-azido-undecane-1-thiol, where each tip created a pattern composed of 16 spots that were printed with identical force and t . The patterning was repeated at t ranging from 0 to 600 s and P ranging from 0.1–7.95 MPa. The force was measured as described previously³³ and then converted to P by the method of Mullen and Basche.^{20,31} Cyclic voltammetry (CV) was used to characterize reactions between **2** and the azide SAMs because the characteristic fc peaks make the

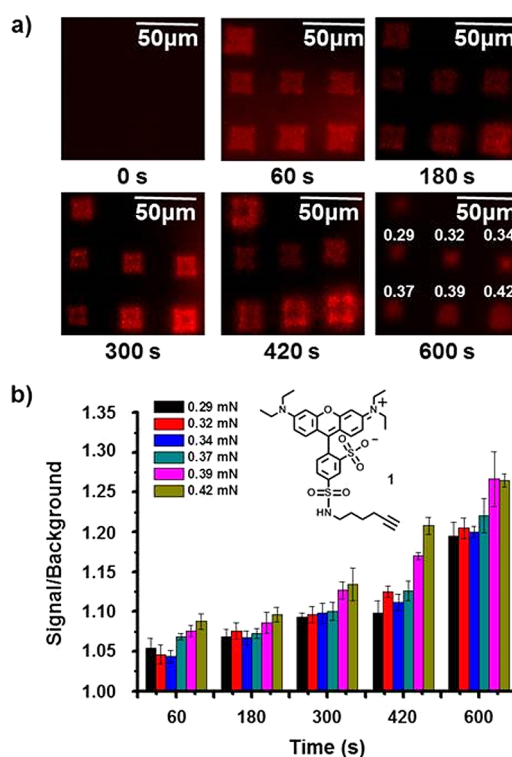


Figure 2. (a) Fluorescent images of 2×3 dot arrays of **1** printed at different t (0, 60, 180, 300, 420, 600 s) and P (0.29, 0.32, 0.34, 0.37, 0.39, 0.42 MPa). (b) Signal-to-background of the printed features of **2** increases with P and t . Error values were determined from three independent measurements.

presence of **2** easy to identify, and CV provides quantitative data on the surface density within the printed features and can also be used to confirm covalent immobilization on conductive surfaces.³⁵ For all printing t and P above 0 s and 0.1 MPa, a redox wave indicative of the fc/fc^+ redox couple was observed. The linear plots of $\ln(\text{scan rate})$ vs $\ln(\text{current})$ further confirmed that the molecules were surface confined as a result of triazole formation.³⁵ A quantitative analysis of the surface density of fc as a function of t and P (Figure 3a) revealed that conversion increases with both increasing P and increasing t . As long as some force is applied, the reaction proceeds to near completion given long enough time to react. However, in the absence of force or very short t (<150 s), no triazole formation was observed. The linear fits of $\ln([\text{azide}])$ for a given P provide the different k , which represents the rate of loss of azide on the surface, because we assume that the reaction follows pseudo-first order kinetics, where **2** is present in large excess. The initial concentration of azide, N_3 , is based on the number of possible fc units that can be immobilized in a well-organized monolayer, which is 2.7×10^{14} molecules per cm^2 .³⁵ It should be noted that when printing under high force, fc surface densities as high as 4.3×10^{14} molecules per cm^2 have been observed,^{35–37} and this discrepancy has been explained by suggesting that subsurface fc is embedded within the monolayer,³⁷ but in our experiments no surface densities above 2.7×10^{14} molecules per cm^2 were detected. The value of k ranges from $2.89 \pm 0.39 \times 10^{-3} \text{ s}^{-1}$ for a P of 2.72 ± 0.21 MPa to $4.52 \pm 0.19 \times 10^{-3} \text{ s}^{-1}$ for a P of 7.95 ± 0.75 MPa (Figure 3b). This sensitive dependence of k on applied P can explain inconsistencies in previous studies on the force dependence of the Huisgen reaction.^{23,25} The applied P must be controlled precisely to achieve full conversion; although seemingly

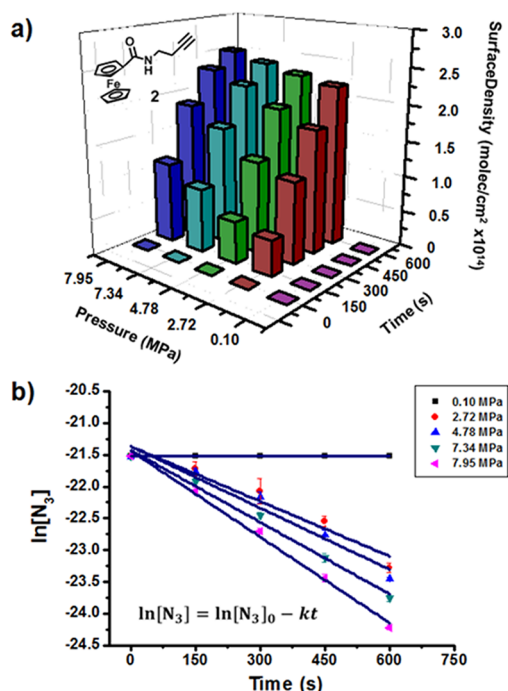


Figure 3. (a) The variation of fc surface density on Au surfaces as a function of P and t . (b) Plots of $\ln([azide])$ to t at different P , whose slope provides k . Error values were determined from three independent measurements.

contradictory, all previous studies on the ability of force to catalyze the Huisgen reaction are likely correct once the role of P on k is accounted for.

A further series of control experiments was performed to confirm the covalent immobilization. Ferrocenecarboxylic acid, which does not react with N_3 , was dissolved in a PEG matrix and printed onto an azido-functionalized Au surface. After printing at 7.95 MPa for 600 s and washing with EtOH and H_2O , the absence of any remaining fc on the surface was confirmed by CV. To show that the rate acceleration under applied force is not simply a reflection of increased reactant concentration, the reaction configuration was inverted: rather than coat the tips with ink and bring them into contact with the surface, the surfaces were coated with ink, and the tips were used to locally apply pressure. The concentrations of **2** spin coated onto the surfaces were varied over two decades (0.3, 0.6, 3, 15, 30 mM), and in each case the tips were used to apply a P of 4.78 MPa for 300 s to print a 4×4 array. The surfaces were characterized by CV, and no significant differences in the value of k were observed.³¹ We concluded that the reaction was zero order in alkyne when present in great excess.

The CV studies were used to determine the V_{obs}^\ddagger (observed dependence of $\ln k$ on pressure) by plotting $\ln k$ versus P (Figure 4a).³⁸ An activation volume of $-189 \pm 41 \text{ cm}^3 \text{ mol}^{-1}$ was determined for the Huisgen cycloaddition on the C11 11-azido-undecane-1-thiol SAM. Calculations at the M06-2X/6-31G(d) level in the gas phase show that the (3 + 2) cycloaddition of alkyl azide and terminal alkyne has a V^\ddagger of about $-13 \text{ cm}^3 \text{ mol}^{-1}$.³¹ This value is significantly smaller than that observed in the experiment.

We attribute the difference between these two values to the monolayer compression that occurs during printing. We propose that the observed activation volume V_{obs}^\ddagger in the nanoreactor is

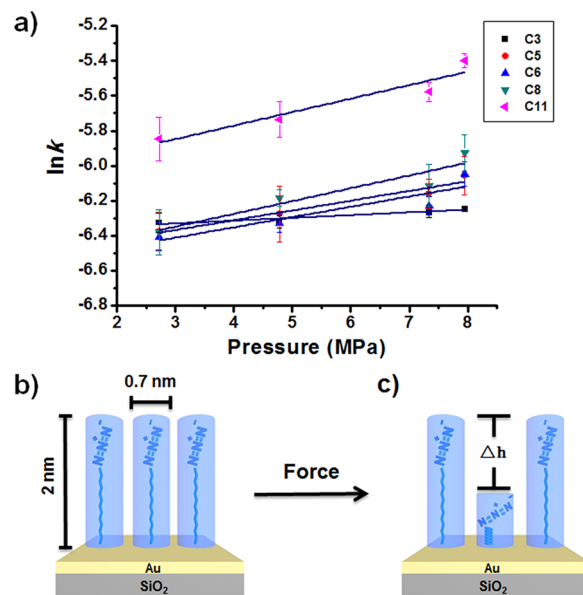


Figure 4. (a) Plot of $\ln k$ vs P at different alkyl chain lengths, whose slope provides V_{obs}^\ddagger . Error values were determined from three independent measurements. (b) Rotation of the C11 azide molecule sweeps out a large cylinder. (c) Monolayer is compressed when tips are brought into contact with surface, decreasing the cylinder volume in the reaction.

the sum of the activation volume of the cycloaddition reaction V_c^\ddagger and the change in the volume of the monolayer ΔV_m (eq 2).

$$V_{obs}^\ddagger = V_c^\ddagger + \Delta V_m \quad (2)$$

To test this hypothesis, we reasoned that the height of the monolayer would alter V_{obs}^\ddagger because of the differences in the change of ΔV_m during compression. Therefore, **2** was printed on SAMs containing alkane chains of different length between the thiol and the azide with a printing time of 5 min and at pressures of 2.72–7.95 MPa (Figure 4a). Based on a maximum packing density of 2.7×10^{14} molecules per cm^2 , the measured V_{obs}^\ddagger decreases gradually from $-189 \text{ cm}^3 \text{ mol}^{-1}$ for an undecyl chain to $-39 \text{ cm}^3 \text{ mol}^{-1}$ for a propyl chain (Table 1).³¹ This indicates that, assuming that V_c^\ddagger remains constant ($-13 \text{ cm}^3 \text{ mol}^{-1}$), the volume change of the monolayer ΔV_m becomes smaller and smaller with the decrease of the height of the monolayer. A simple model can semiquantitatively account for the change in ΔV_m (Figure 4b). The free rotation of the C11 azide molecule on Au in a standing up configuration³⁶ sweeps out a cylinder. From

Table 1. Observed Activation Volumes from Experiments and Calculations for the Huisgen Reaction on Monolayers with Different Alkane Chain Lengths

| alkane chain length of $N_3(CH_2)_nSH$ | experimental activation volume (cm^3/mol) ^{a,b} | computed activation volume (cm^3/mol) ^b |
|--|--|--|
| C11 | -189 ± 41 | -191 |
| C8 | -179 ± 45 | -169 |
| C6 | -144 ± 45 | -147 |
| C5 | -137 ± 21 | -124 |
| C3 | -39 ± 9 | -91 |

^aError values were determined from three independent measurements.

^bCalculated values are a combination of the activation volume of the cycloaddition reaction V_c^\ddagger ($-13 \text{ cm}^3/\text{mol}$) and the change in the volume of the monolayer ΔV_m . Maximum possible surface density was calculated as 2.7×10^{14} molecules per cm^2 .³¹

the density of 2.7×10^{14} molecules/cm² of the C11 chain on the surface,³⁵ the occupied area of the single molecule is calculated to be 0.37 nm². The height of the C11 monolayer is about 2.0 nm,³¹ so the volume of the cylinder is 0.74 nm³ or 445 cm³ mol⁻¹. Calculations indicate that, when two anti conformers in the middle of the alkane chain are changed to gauche in the reaction, the height of the C11 monolayer decreases to 1.2 nm.³¹ This will result in a Δh (Figure 4c) of -0.8 nm, leading to an ΔV_m of -0.30 nm³ or -178 cm³ mol⁻¹. According to this model, the computed ΔV_m values for the C8, C6, C5, and C3 monolayers are -156, -134, -111, and -78 cm³ mol⁻¹, respectively,³¹ and these data reproduce the trend observed in the experiments (Table 1). The largest discrepancy between experimental and computational values occurs with the C3 monolayers, which are more likely to lie flat on the substrate and are therefore less compressible along the force vector than the closely packed monolayers used for computations.

In conclusion, we have used massively parallel tip arrays to form nanoreactors that can apply force to accelerate bond-forming reactions with negative V^\ddagger on surfaces. This approach was used to show that the velocity of the Huisgen reaction on surfaces is sensitively dependent on force and monolayer chain length, and a semiquantitative model was developed that explains the previous contradictory results in the literature. Force may have an important role in many interfacial processes, and the approach described in this work can be used to address challenges in materials science, biology, and nanotechnology.

■ ASSOCIATED CONTENT

● Supporting Information

Experimental details and computational data. This material is available free of charge via the Internet at <http://pubs.acs.org>.

■ AUTHOR INFORMATION

Corresponding Author

a.braunschweig@miami.edu

Notes

The authors declare no competing financial interest.

■ ACKNOWLEDGMENTS

A.B.B. is grateful to the Air Force Office of Scientific Research (Young Investigator Award FA9550-13-1-0188) and the National Science Foundation (DBI-1340038), and K.N.H. is grateful to the National Science Foundation (CHE-1059084) for financial support. Calculations were performed on the Extreme Science and Engineering Discovery Environment (XSEDE), which is supported by the NSF (OCI-1053575).

■ REFERENCES

- (1) Kuster, C. J. T.; Scheeren, H. W. In *High Pressure Chemistry*; van Eldik, R., Klaerner, F.-G., Eds.; Wiley-VCH: Weinheim, 2007; pp 284–304.
- (2) Blandamer, M. J.; Burgess, J.; Robertson, R. E.; Scott, J. M. W. *Chem. Rev.* **1982**, *82*, 259.
- (3) Ribas-Arino, J.; Marx, D. *Chem. Rev.* **2012**, *112*, 5412.
- (4) Beyer, M. K.; Clausen-Schaumann, H. *Chem. Rev.* **2005**, *105*, 2921.
- (5) Wiggins, K. M.; Brantley, J. N.; Bielawski, C. W. *Chem. Soc. Rev.* **2013**, *42*, 7130.
- (6) Caruso, M. M.; Davis, D. A.; Shen, Q.; Odom, S. A.; Sottos, N. R.; White, S. R.; Moore, J. S. *Chem. Rev.* **2009**, *109*, 5755.
- (7) Brantley, J. N.; Wiggins, K. M.; Bielawski, C. W. *Science* **2011**, *333*, 1606.
- (8) Lenhardt, J. M.; Ong, M. T.; Choe, R.; Evenhuis, C. R.; Martinez, T. J.; Craig, S. L. *Science* **2010**, *329*, 1057.
- (9) Hickenboth, C. R.; Moore, J. S.; White, S. R.; Sottos, N. R.; Baudry, J.; Wilson, S. R. *Nature* **2007**, *446*, 423.
- (10) Larsen, M. B.; Boydston, A. J. *J. Am. Chem. Soc.* **2013**, *135*, 8189.
- (11) Kersey, F. R.; Yount, W. C.; Craig, S. L. *J. Am. Chem. Soc.* **2006**, *128*, 3886.
- (12) Black, A. L.; Orlicki, J. A.; Craig, S. L. *J. Mater. Chem.* **2011**, *21*, 8460.
- (13) Todres, Z. V. *Organic Mechanochemistry and Its Practical Applications*; CRC Press: Boca Raton, FL, 2006.
- (14) Fanselow, D. L.; Drickamer, H. G. *J. Chem. Phys.* **1974**, *61*, 4567.
- (15) Wilson, D. G.; Drickamer, H. G. *J. Chem. Phys.* **1975**, *63*, 3649.
- (16) Kawamura, I.; Degawa, Y.; Yamaguchi, S.; Nishimura, K.; Tuzi, S.; Saito, H.; Naito, A. *Photochem. Photobiol.* **2007**, *83*, 346.
- (17) Tabata, M.; Tanaka, Y.; Sadahiro, Y.; Sone, T.; Yokota, K.; Miura, I. *Macromolecules* **1997**, *30*, 5200.
- (18) Bian, S. D.; Scott, A. M.; Cao, Y.; Liang, Y.; Osuna, S.; Houk, K. N.; Braunschweig, A. B. *J. Am. Chem. Soc.* **2013**, *135*, 9240.
- (19) Paxton, W. F.; Spruell, J. M.; Stoddart, J. F. *J. Am. Chem. Soc.* **2009**, *131*, 6692.
- (20) Stottinger, S.; Hinze, G.; Diezemann, G.; Oesterling, I.; Mullen, K.; Basche, T. *Nat. Nanotechnol.* **2014**, *9*, 182.
- (21) Brantley, J. N.; Bailey, C. B.; Wiggins, K. M.; Keatinge-Clayth, A. T.; Bielawski, C. W. *Polym. Chem.* **2013**, *4*, 3916.
- (22) Lantz, M. A.; Hug, H. J.; Hoffmann, R.; van Schendel, P. J. A.; Kappenberger, P.; Martin, S.; Barato, A.; Guntherodt, H. J. *Science* **2001**, *291*, 2580.
- (23) Mehlich, J.; Ravoo, B. J. *Org. Biomol. Chem.* **2011**, *9*, 4108.
- (24) Spruell, J. M.; Sheriff, B. A.; Rozkiewicz, D. I.; Dichtel, W. R.; Rohde, R. D.; Reinhoudt, D. N.; Stoddart, J. F.; Heath, J. R. *Angew. Chem., Int. Ed.* **2008**, *47*, 9927.
- (25) Rozkiewicz, D. I.; Janczewski, D.; Verboom, W.; Ravoo, B. J.; Reinhoudt, D. N. *Angew. Chem., Int. Ed.* **2006**, *45*, 5292.
- (26) Huo, F. W.; Zheng, Z. J.; Zheng, G. F.; Giam, L. R.; Zhang, H.; Mirkin, C. A. *Science* **2008**, *321*, 1658.
- (27) Eichelsdoerfer, D. J.; Liao, X.; Cabezas, M. D.; Morris, W.; Radha, B.; Brown, K. A.; Giam, L. R.; Braunschweig, A. B.; Mirkin, C. A. *Nat. Protoc.* **2013**, *8*, 2548.
- (28) Giam, L. R.; Mirkin, C. A. *Angew. Chem., Int. Ed.* **2011**, *50*, 7482.
- (29) Braunschweig, A. B.; Huo, F. W.; Mirkin, C. A. *Nat. Chem.* **2009**, *1*, 353.
- (30) Huang, L.; Braunschweig, A. B.; Shim, W.; Qin, L. D.; Lim, J. K.; Hurst, S. J.; Huo, F. W.; Xue, C.; Jong, J. W.; Mirkin, C. A. *Small* **2010**, *6*, 1077.
- (31) See Supporting Information for details.
- (32) Bian, S. D.; He, J. J.; Schesing, K. B.; Braunschweig, A. B. *Small* **2012**, *8*, 2000.
- (33) Liao, X.; Braunschweig, A. B.; Zheng, Z. J.; Mirkin, C. A. *Small* **2010**, *6*, 1082.
- (34) Liao, X.; Braunschweig, A. B.; Mirkin, C. A. *Nano Lett.* **2010**, *10*, 1335.
- (35) Chidsey, C. E. D.; Bertozzi, C. R.; Putvinski, T. M.; Muijsce, A. M. *J. Am. Chem. Soc.* **1990**, *112*, 4301.
- (36) Vericat, C.; Vela, M. E.; Benitez, G.; Carro, P.; Salvarezza, R. C. *Chem. Soc. Rev.* **2010**, *39*, 1805.
- (37) Pellow, M. A.; Stack, T. D. P.; Chidsey, E. D. C. *Langmuir* **2013**, *29*, 5383.
- (38) Jezowski, S. R.; Zhu, L. Y.; Wang, Y. B.; Rice, A. P.; Scott, G. W.; Bardeen, C. J.; Chronister, E. L. *J. Am. Chem. Soc.* **2012**, *134*, 7459.